Geochemical Journal, Vol. 46, pp. 89 to 106, 2012

Methane production and accumulation in the Nankai accretionary prism: Results from IODP Expeditions 315 and 316

TOMOHIRO TOKI,[1]* YUTO UEHARA,[1] KAZUNARI KINJO,[1] AKIRA IJIRI,[2] URUMU TSUNOGAI,[3] HITOSHI TOMARU[4] and JUICHIRO ASHI[5]

[1]Department of Chemistry, Biology and Marine Science, Faculty of Science, University of the Ryukyus, 1 Senbaru, Nishihara, Okinawa 903-0213, Japan
[2]Kochi Institute for Core Sample Research, JAMSTEC, B200, Monobe, Nankoku 783-8502, Japan
[3]Earth and Planetary System Science, Faculty of Science, Hokkaido University, N10 W8, Kita-ku, Sapporo, Hokkaido 060-0810, Japan
[4]Department of Earth and Planetary Science, Graduate School of Science, The University of Tokyo, 7-3-1 Hongo, Bunkyo-ku, Tokyo 113-0033, Japan
[5]Department of Ocean Floor Geoscience, Atmosphere and Ocean Research Institute, The University of Tokyo, 5-1-5 Kashiwanoha, Kashiwa, Chiba 277-8568, Japan

(*Received July 1, 2011; Accepted November 30, 2011*)

Pore waters were taken from core sediments of Sites C0001, C0004, and C0008 on the landward slope of the Nankai Trough and Site C0002 in the forearc basin of the Nankai accretionary prism off Kumano during Integrated Ocean Drilling Program Expeditions 315 and 316. The carbon isotopic ratios of CH_4 and total carbon dioxide ($\sum CO_2$) in dissolved gases were measured. The contribution of thermogenic CH_4 was negligible at all sites, while carbon isotopic separation between CH_4 and $\sum CO_2$ indicated that CH_4 formation was mainly by microbial hydrogenotrophic methanogenesis. Evaluation of the isotopic fraction of the initial substrate $\sum CO_2$ pool showed larger fractionation at Site C0002 than at the other sites in the transect. In addition, the NH_4^+ concentration was higher at Site C0002 than at the other sites, indicating that organic matter degradation occurred more actively at Site C0002 than at the other sites. Therefore, CO_2 and H_2 as well as NH_4^+ were actively generated by the organic matter degradation at Site C0002, which could stimulate methanogenesis utilizing CO_2 and H_2 as substrates at Site C0002. The high sedimentation rate at Site C0002 in the forearc basin was due to the geomorphological setting of the site, within the outer ridge rimming the sediment-filled Kumano Basin, leading to organic matter burial without aerobic degradation on the surface of the seafloor, which preserve labile organic matter for utilization by methanogenesis. On the other hand, slope sediments were already exposed by organic matter degradation, which leaves scarce labile organic matter for supporting CH_4 generation. Geomorphology was possibly an important factor controlling CH_4 formation and accumulation, and the Kumano Basin sediments have greater potential as a CH_4 hydrate reservoir than the landward slope sediments in the Nankai accretionary prism off Kumano.

Keywords: Nankai accretionary prism, IODP, origin of methane, carbon isotope, methanogenesis

INTRODUCTION

The Nankai Trough is a convergent plate margin (Fig. 1a) where the Philippine Sea plate is subducting northwestward beneath the Eurasian plate at a convergent rate of about 4 mm/yr (Seno *et al*., 1993). Shikoku basin sediments on the Philippine Sea plate are actively accreting on the landward slope of the Nankai Trough (Fig. 1b). A splay fault, identified by using reflection seismic images, intersects the seafloor of the Nankai accretionary prism along the landward slope off Kumano, Japan ("megasplay fault"; Fig. 3; Park *et al*., 2002). At the top of the slope, a continuous pronounced outer ridge has developed that corresponds to the seaward boundary of the forearc basin, the "Kumano Basin", which is filled with terrigenous sediments (Fig. 3; Moore *et al*., 2001). Beneath the landward slope in the Nankai Trough off Kumano and the Kumano Basin, an anomalous reflector running parallel to the seafloor known as the bottom-simulating reflector (BSR) has been observed (Kinoshita *et al*., 2009). This reflector has been recognized as a high-velocity layer of gas hydrate underlying low-velocity gas-bearing sediments (Shipley *et al*., 1979). Indeed, the chemical and isotopic compositions of the pore waters imply the presence of gas hydrates in the sediments (Kinoshita *et al*., 2009).

*Corresponding author (e-mail: toki@sci.u-ryukyu.ac.jp)

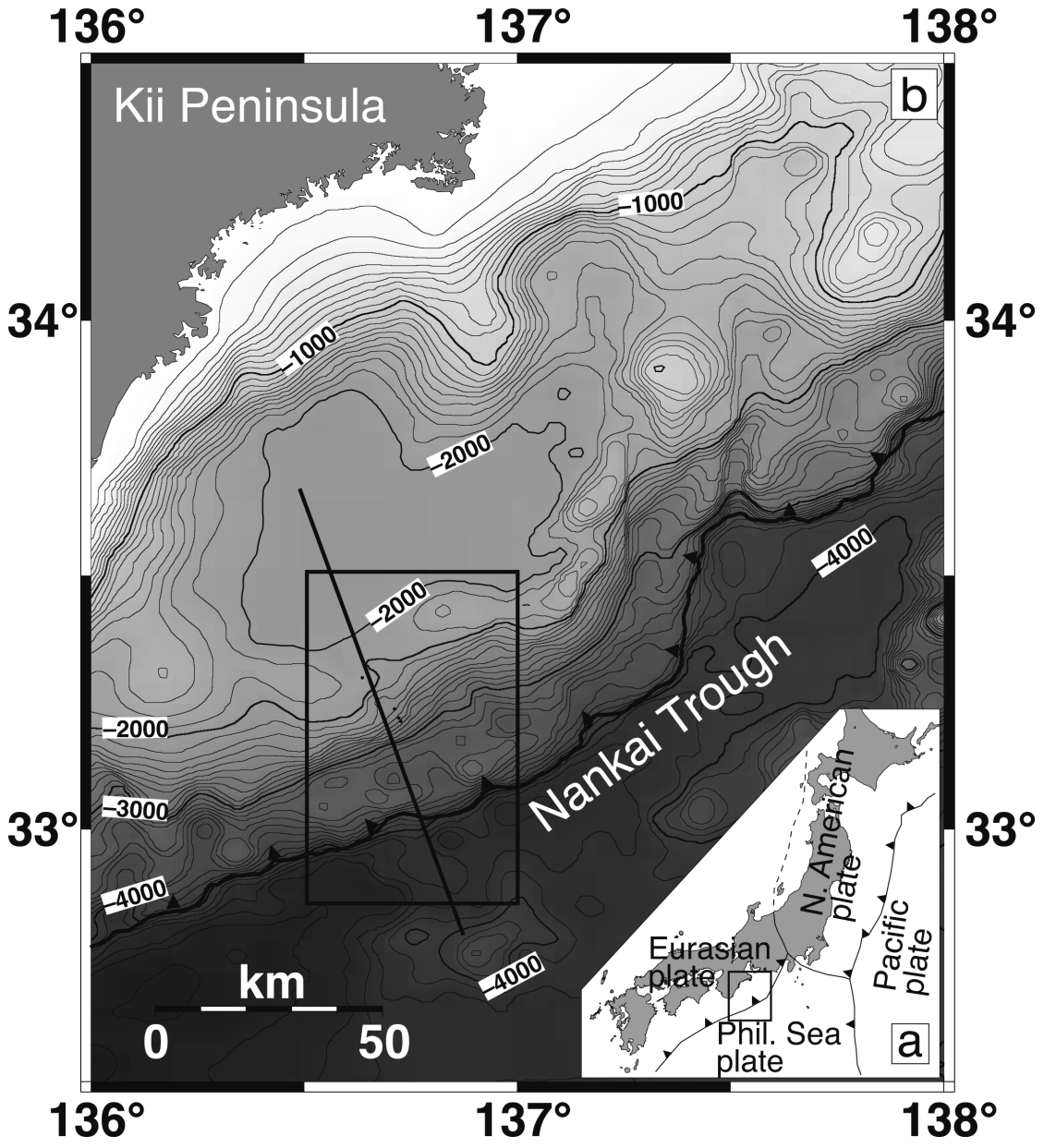

Fig. 1. (a) Simplified tectonic map of the Nankai Trough off Kumano showing the regional plate tectonic setting. The box indicates the location of (b). (b) Bathymetry of the studied region, showing the regional setting of the IODP drilling transect during IODP Expeditions 315 and 316. The box indicates the location of Fig. 2, and the solid line shows the location of the seismic cross section in Fig. 3.

Under conditions of low temperature and high pressure, the CH_4 concentration exceeds CH_4 solubility in pore water, and a massive reservoir of CH_4 as CH_4 clathrate hydrate can form (Kvenvolden, 1993; Xu and Ruppel, 1999); such reservoirs are of great interest as a possible future energy source (e.g., Kvenvolden, 1988). Furthermore, CH_4 is a strong greenhouse gas, 21 times more potent a greenhouse gas than CO_2 (Mitchell, 1989). The occasional CH_4 release from a vast reservoir of sediment-hosted CH_4 hydrates may have driven rapid climate change during several periods of Earth's history (e.g., Dickens *et al*., 1997; Kennett *et al*., 2003). Actually, CH_4-charged fluids would migrate upward from sedimentary reservoirs into subsurface sediments, and are seeping from the seafloor, thereby supplying benthic biological assemblages with chemosynthetic microbes along the scarp base of the megasplay fault and at mud volcanoes in the Kumano Basin (Toki *et al*., 2004; Ijiri, 2003). It is impor-

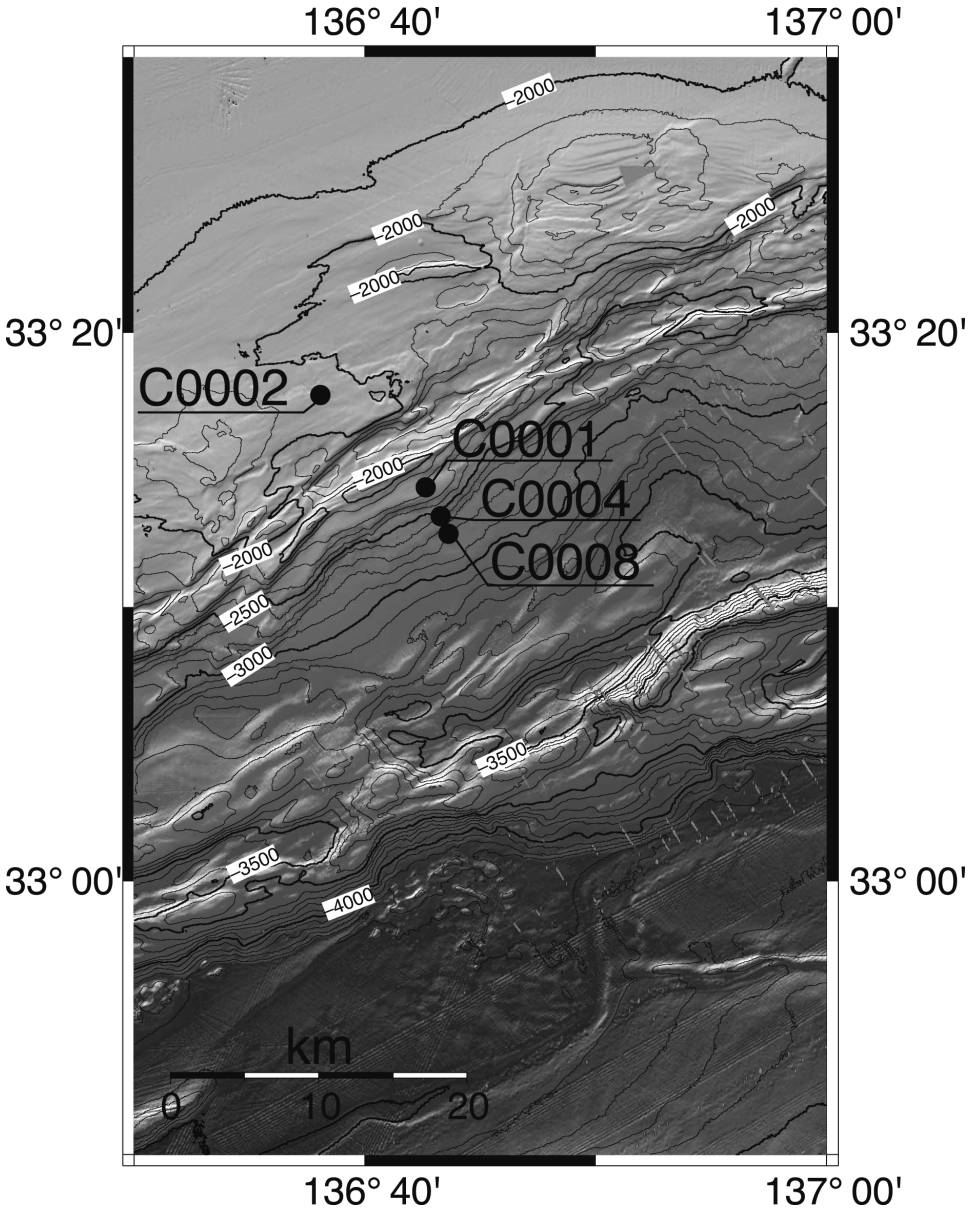

Fig. 2. Site map for IODP Expeditions 314, 315, and 316. The solid circles show the locations of the IODP drill Sites C0001, C0002, C0004, and C0008.

tant to understand the distribution of CH_4 reservoir for potential energy resource as well as potential role in future climate change, but the primary factors leading to the formation and accumulation of CH_4 are poorly understood.

With respect to CH_4 accumulation, CH_4 migration from greater depth by higher rates or *in situ* CH_4 generation by higher rates has been an important factor (Malinverno *et al*., 2008). The evidence of CH_4 migration has been the distribution of deep-sourced materials in CH_4 reservoirs (Egeberg and Dickens, 1999; Fehn *et al*., 2000) or the excess of CH_4 in the reservoirs than that expected by calculation allowing for only *in situ* CH_4 generation (Hyndman and Davis, 1992; Waseda and Uchida, 2004). On the other hand, the importance of *in situ* CH_4 generation has been suggested by applying Rayleigh distillation model to the observed profiles of carbon isotopic composition of CH_4 (Claypool and Kaplan, 1974; Galimov and Kvenvolden, 1983). Pohlman *et al*. (2009) investigated CH_4 distribution within the northern Cascadia margin accretionary prism, and suggested that higher sedimentation rates reduce the chance of sedimentary organic matter degradation during burial, leading to multiply the availability of organic matter to

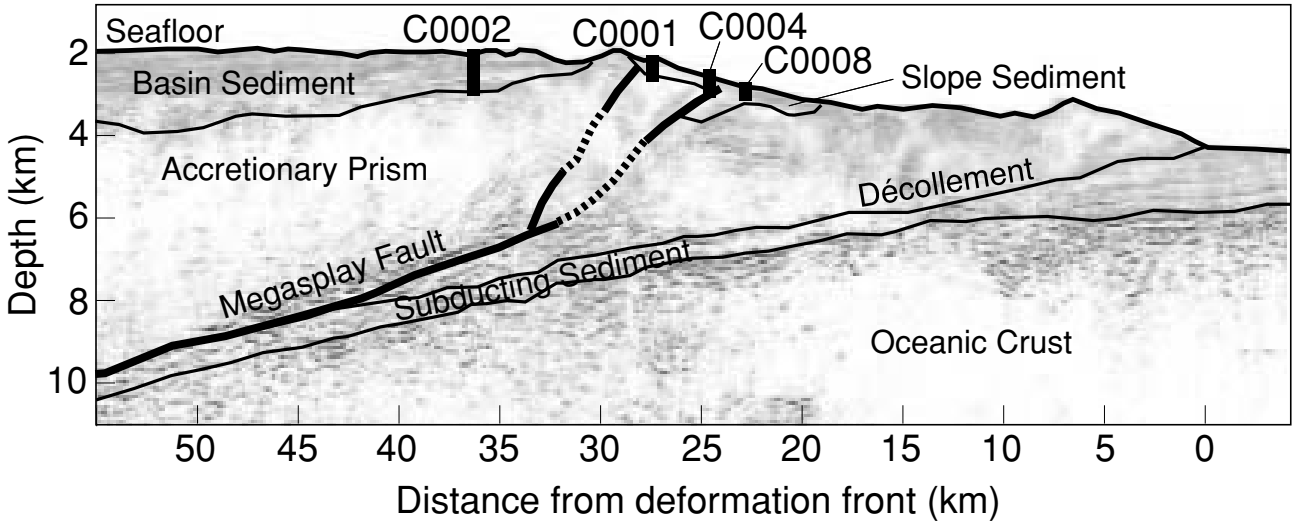

Fig. 3. Interpretation of a seismic cross section through IODP Sites C0001, C0002, C0004, and C0008 (modified from Moore et al., 2009). The location of the section is shown in Fig. 1b. The bold dotted lines show the trace of the megasplay faults.

generate CH_4, so they concluded that higher sedimentation rates are the most important factor for the CH_4 accumulation.

CH_4 in sedimentary reservoirs can be produced either through microbial processes during methanogenesis or by the thermal degradation of organic matter. Microbial CH_4 is generated in shallow sediments by methanogenic *Archaea* primarily through two processes (Jeris and McCarty, 1965; Smith and Mah, 1966; Hungate, 1967; Cappenberg and Prins, 1974). Microbial hydrogenotrophic methanogenesis, which is coupled to the oxidation of hydrogen molecules, generally dominates methanogenesis in oligotrophic marine sediments (Eq. (1)), whereas acetoclastic methanogenesis, in which acetate is fermented to CO_2 and CH_4, is the dominant formation pathway in freshwater systems (Eq. (2)) (Whiticar *et al.*, 1986).

$$CO_2 + 4H_2 \rightarrow CH_4 + 2H_2O \quad (1)$$

$$CH_3COOH \rightarrow CH_4 + CO_2. \quad (2)$$

Some methanogens can also use methanol and methylamines (Oremland *et al.*, 1982; Oremland and Polcin, 1982), although these substances are thought to make minor contributions to methanogenesis under natural environments (Lovley and Klug, 1986). Recently, carbon isotopic compositions of acetate have indicated that acetoclastic methanogenesis occurs in marine sediments as well (Wellsbury *et al.*, 1997; Heuer *et al.*, 2009). However, carbon isotopic compositions of CO_2 and CH_4 are controlled by microbial hydrogenotrophic methanogenesis, which is a relatively important process in the carbon cycle, as demonstrated by Wellsbury *et al.* (1997) and Heuer *et al.* (2009).

On the other hand, thermogenic CH_4 is formed as an end product when sedimentary organic matter thermally degrades in deep sediments (Eq. (3)).

$$R\text{–}COOH \rightarrow R\text{–}H + CO_2 \quad (3)$$

where R represents an alkyl group (e.g., Schoell, 1980). Thermogenic CH_4 formation occurs at temperatures higher than about 80°C (e.g., Quigley and Mackenzie, 1988), which generally occur only at great depth in sediments, in case of the Nankai accretionary prism off Kumano below about 2 km depending on geothermal gradient which were observed from 43 to 52°C/km during IODP Expeditions 315 and 316 (Kinoshita *et al.*, 2009). Several previous drilling programs have revealed the occurrence of thermogenic CH_4 at great depth in sediments (e.g., Berner and Faber, 1993; Waseda and Uchida, 2004).

In the Nankai accretionary prism, the distribution of CH_4 has been revealed at Sites 582 and 583 off Ashizuri,

Fig. 4. Depth profiles of Sites C0001, C0002, C0004, and C0008 showing (a) pore water Cl^- concentration; (b) $\delta^{18}O$ of pore water; (c) pore water CH_4 concentration; (d) C_1/C_2 ratio. Note that the difference in the depth ranges: 1200 m in the Site C0002 profile and 500 m in the other profiles.

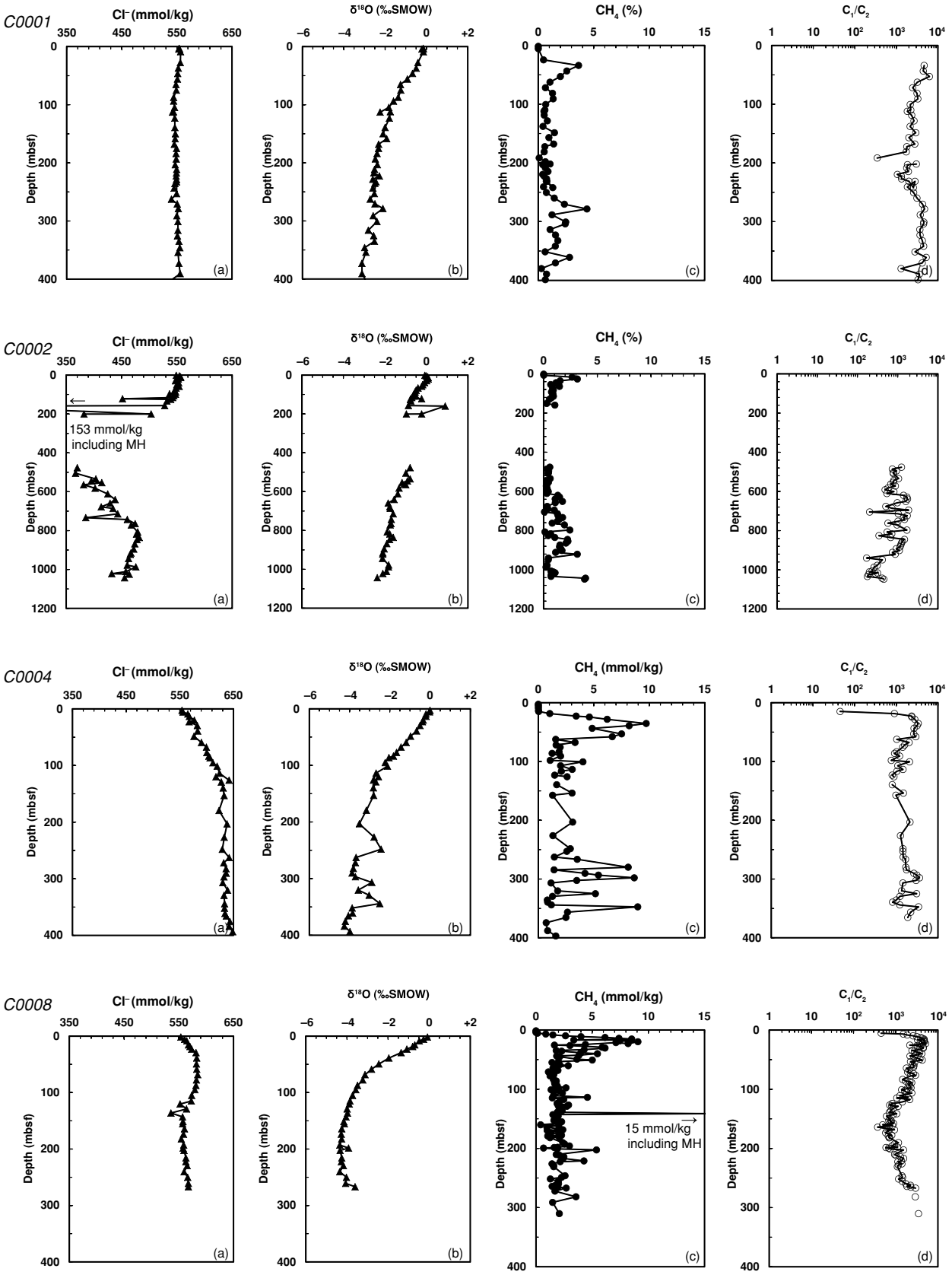
C0001
Cl⁻ (mmol/kg)
δ18O (‰SMOW)
CH4 (%)
C1/C2
Depth (mbsf)
(a)
(b)
(c)
(d)
C0002
153 mmol/kg
including MH
C0004
CH4 (mmol/kg)
C0008
15 mmol/kg
including MH

Fig. 4.

Table 1(a). $\delta^{13}C$ of ΣCO_2 and CH_4 in pore water samples, Site C0001

Hole	Core	Section	Depth mbsf	$\delta^{13}C$–ΣCO_2 ‰PDB	$\delta^{13}C$–CH_4 ‰PDB
C0001E					
	1H	4	3.0	–20.6	N.D.
	1H	6	3.9	–25.3	–75.0
	1H	7	4.1	–26.5	–77.7
	2H	4	8.7	–37.5	–74.6
	4H	4	27.5	–25.1	–87.8
	5H	4	37.0	–13.2	–82.6
	6H	4	46.2	–6.1	–80.9
	7H	4	55.8	–2.7	–77.2
	8H	4	65.2	0.3	–77.6
	9H	4	74.9	1.7	–74.0
	10H	7	87.3	3.1	–74.7
	11H	4	93.7	4.1	–71.9
	12H	5	104.6	4.7	–67.2
	13H	4	112.8	5.2	–71.1
C0001F					
	1H	4	112.1	4.0	–73.6
	2H	5	123.0	4.9	–74.1
	4H	3	139.2	5.5	–71.4
	5H	4	150.0	5.7	–67.8
	6H	4	158.5	5.2	–69.8
	7H	12	168.0	6.0	–68.0
	8H	4	175.1	5.8	–66.2
	9H	4	184.0	5.3	–67.1
	10H	10	193.4	4.0	–70.5
	13H	2	203.2	4.1	–70.1
	14H	4	211.3	4.0	–67.9
	15H	4	217.3	5.6	–67.7
	18H	4	222.7	3.8	–67.7
	19H	4	228.3	5.4	–69.9
	20X	5	235.3	4.1	–73.2
	21X	4	243.4	3.7	–72.1
C0001H					
	1R	3	232.6	4.1	–71.5
	3R	4	253.0	4.1	–70.5
	4R	4	262.5	3.4	–71.5
	5R	3	270.6	11.6	–69.6
	6R	2	278.7	3.5	–72.3
	7R	4	291.1	3.6	–69.4
	8R	4	300.9	3.1	–69.4
	10R	4	316.1	2.2	–74.5
	11R	4	325.5	5.8	–73.0
	12R	4	335.1	1.4	–74.7
	13R	5	345.9	1.8	–74.1
	14R	4	354.0	1.9	–69.3
	16R	4	373.0	1.1	–71.8
	19R	3	400.1	1.8	–71.4
	21R	3	415.1	3.4	–68.2
	23R	2	430.6	0.9	N.D.
	24R	2	440.1	–1.5	N.D.

Table 1(b). $\delta^{13}C$ of ΣCO_2 and CH_4 in pore water samples, Site C0002

Hole	Core	Section	Depth mbsf	$\delta^{13}C$–ΣCO_2 ‰PDB	$\delta^{13}C$–CH_4 ‰PDB
C0002D					
Unit I	1H	2	1.5	–12.8	–71.3
	1H	5	4.3	–34.7	N.D.
	2H	3	8.8	–43.0	N.D.
	2H	7	13.1	–29.7	–82.9
	3H	4	19.5	–12.8	–79.2
	4H	4	29.2	0.1	N.D.
	5H	4	38.7	6.2	–72.0
	6H	5	49.4	9.5	N.D.
	7H	4	57.7	10.9	–68.6
	8H	4	66.9	11.8	–69.0
	9H	5	78.1	12.1	–67.4
	10H	4	86.2	12.0	–67.0
	11H	5	96.7	12.8	–66.4
	12H	5	106.4	13.0	–65.2
	13H	5	115.8	13.0	–64.3
	14H	3(HYD)	121.9	12.6	–66.6
	14H	5	124.7	13.6	–63.6
	15X	5	133.2	13.6	–65.7
Unit II	16H	6	157.1	14.7	–64.7
	17X	4(HYD)	159.8	13.4	–66.7
	18H	1(HYD)	200.4	13.0	–65.0
	18H	2	200.6	14.2	–61.5
C0002B					
	1R	2	476.6	14.7	–53.8
	4R	2	504.8	14.4	–49.7
	10R	2	553.6	12.9	–59.5
	11R	3	564.5	12.0	–59.2
	13R	2	582.1	11.3	–57.4
	19R	3	640.5	10.6	–55.4
	21R	3	659.1	9.1	–55.5
	23R	3	678.0	8.3	–59.6
	24R	2	686.1	7.5	N.D.
	27R	2	714.3	7.5	–57.2
	30R	2	743.1	4.8	–57.4
	32R	5	764.5	5.7	–60.3
	33R	2	771.2	10.4	N.D.
	37R	2	807.1	5.0	–62.3
Unit III	40R	2	835.6	2.1	–63.3
	41R	3	846.5	1.5	–61.6
	43R	5	868.0	–0.2	–60.6
	46R	4	895.0	0.2	–60.0
	48R	5	915.4	–0.3	–60.8
Unit IV	49R	3	922.1	–0.5	N.D.
	51R	5	943.9	–0.6	–62.5
	55R	2	977.7	–1.9	N.D.
	56R	2	986.8	N.D.	–60.9
	62R	2	1024.2	–4.8	–58.9

drilled during Deep Sea Drilling Project Leg 87 (Claypool *et al.*, 1986), at Site 808 off Muroto, drilled during Ocean Drilling Program Leg 131 (Berner and Faber, 1993), and in the MITI well off Tokai (Waseda and Uchida, 2004). At all three localities, the chemical and isotopic composition of sampled core void gas or pressure core gas has

Table 1(c). $\delta^{13}C$ of ΣCO_2 and CH_4 in pore water samples, Site C0004

Hole	Core	Section	Depth mbsf	$\delta^{13}C$–ΣCO_2 ‰PDB	$\delta^{13}C$–CH_4 ‰PDB
C0004C					
Unit I	1H	3	2.7	–20.1	–85.3
	4H	4	29.5	–31.1	–85.3
	5H	4	39.2	–16.3	–81.9
	6H	4	48.6	–7.4	–79.9
	7H	6	59.4	–1.3	–76.4
	8H	4	67.7	0.7	–75.2
	9H	4	77.3	2.7	–72.6
Unit II	10H	3	83.6	3.9	–72.4
	11H	2	86.4	3.9	–72.5
	12X	6	95.1	4.7	–69.5
C0004D					
	5R	3	139.7	6.2	–68.7
	13R	2	179.5	5.9	–69.7
	16R	2	203.2	4.7	–68.9
Unit III	32R	3	290.2	6.1	–67.5
Unit IV	44R	3	344.2	5.9	N.D.
	46R	2	352.1	N.D.	–66.4
	48R	2	361.2	5.9	–63.1
	51R	2	375.6	4.9	–60.7
	53R	2	384.1	5.5	–65.1
	55R	2	393.6	5.2	–64.9

Table 1(d). $\delta^{13}C$ of ΣCO_2 and CH_4 in pore water samples, Site C0008

Hole	Core	Section	Depth mbsf	$\delta^{13}C$–ΣCO_2 ‰PDB	$\delta^{13}C$–CH_4 ‰PDB
C0008A					
Unit I	1H	3	1.7	–31.7	–89.5
	1H	7	5.5	–52.0	–110.1
	2H	2	8.5	–41.8	–108.1
	2H	8	15.5	–29.0	–81.3
	3H	3	18.5	0.6	–78.9
	3H	8	23.1	–17.0	–99.9
	4H	4	29.3	2.3	–74.9
	5H	4	38.8	–4.7	–70.8
	6H	5	49.4	4.8	N.D.
	7H	5	58.7	–1.1	–71.8
	8H	5	68.4	1.2	–70.2
	9H	5	77.7	6.6	–71.0
	10H	6	87.4	6.8	–70.1
	11H	4	94.9	6.5	–69.7
	12H	5	105.1	6.7	–67.5
	13H	5	114.9	9.8	–69.4
	15H	2	120.3	6.7	–70.4
	16H	4	129.0	6.8	–66.3
	17H	6	136.3	9.8	–67.5
	18H	3	143.2	6.8	–68.0
	19H	2	151.5	6.9	–65.7
	20H	3	155.2	5.2	–66.1
	22H	6	173.8	6.6	–62.3
	23H	5	182.2	–2.4	–65.4
	24H	6	192.9	–1.2	–65.6
	25H	2	198.4	8.0	–66.9
	26H	2	202.4	7.4	–64.4
	27H	5	215.8	7.3	–67.4
	28H	3	222.4	7.1	–64.9
	29X	5	229.4	7.0	–66.7
	30X	7	240.3	0.6	–66.7
	31X	6	250.1	5.1	–66.2
	32X	7	260.9	–1.1	–66.7
	33X	4	266.9	8.0	–66.8
C0008C					
	1H	2	1.5	–28.4	–97.9
	1H	5	4.4	–54.1	–109.4
	2H	2	6.9	–46.1	–90.2
	2H	7	12.3	–30.6	–78.9
	3H	3	17.9	–12.9	–76.2
	3H	7	22.1	–2.4	–75.4
	4H	5	29.5	–0.8	N.D.
	5H	5	38.1	–3.4	–72.6
	9H	7	73.1	N.D.	–74.8

N.D. = Not Determined.

demonstrated the presence of microbial gases in the upper about 1000 m, and mixing between microbial and thermogenic gases below ~1000 m at Site 808 and below ~1500 m in the MITI well (Berner and Faber, 1993; Waseda and Uchida, 2004).

Integrated Ocean Drilling Program (IODP) Expeditions 314, 315, and 316 explored the accretionary prism in the Nankai Trough off Kumano (Fig. 2; Kinoshita *et al*., 2009). During Expedition 314, drilling had been carried out at six sites (Sites C0001~C0006). At Site C0002, which is located at the southern margin of the forearc basin, drilling had been carried out for getting the logging-while-drilling (LWD) data, therefore no sediment was sampled (Fig. 3; Kinoshita *et al*., 2008). According to the LWD data gas hydrates have been inferred in the upper ~400 m at Site C0002 (Kinoshita *et al*., 2008). During Expedition 315, two sites (Sites C0001 and C0002) were drilled and sediments were sampled; Site C0001 is located on the hanging wall of the megasplay fault (Fig. 3). During Expedition 316, drilling and sampling had been carried out at four sites (Sites C0004 and C0006~C0008). Site C0004 was drilled at the toe of a thrust wedge in the hanging wall of the megasplay fault system, and Site C0008 was drilled approximately 1 km seaward to investigate the basin seaward of the splay fault at Site C0004 (Fig. 3). During Expedition 315 and 316, pore water were extracted from sediment samples, and concentrations of major components and hydrocarbons in the pore water were measured onboard (Kinoshita *et al*., 2009). Figure 4 are depth profiles of (a) Cl^- concentrations, (b) oxygen isotope ratio ($\delta^{18}O$) of pore water, (c) CH_4 concentrations, and (d) ratio of CH_4 to C_2H_6 (C_1/C_2) reported by Kinoshita *et al*. (2009) in pore water from cores collected at Sites C0001, C0002, C0004, and C0008.

At Site C0002, negative anomalies of Cl^- concentrations in pore water were observed in the layers below 200 mbsf (meters below seafloor) where the occurrence of gas hydrates was inferred by LWD data (Fig. 4a; Kinoshita *et al*., 2009). At Site C0008 within the landward slope in the Nankai accretionary prism, negative excursions was superimposed on smooth profile of Cl^- concentration in pore water around 100 mbsf (Fig. 4a), coinciding with similar minima in the other dissolved elements and maxima in $\delta^{18}O$ of pore water (Fig. 4b), which have indicated the occurrence of gas hydrates in several layers. These coupled anomalies have been used as indicators for the presence of hydrates; hydrates exclude the sea salts from their crystal structure and preferentially uptake ^{18}O of water in the solid phase during the formation (Kvenvolden and Kastner, 1990; Maekawa and Imai, 2000), therefore, hydrate-bearing sediments sampled from deep seafloor embed pore water with Cl^- decrease and ^{18}O enrichment (Hesse and Harrison, 1981; Ussler and Paull, 1995). Such chemical and isotopic features of pore waters were not found in sediments from Site C0004 (Fig. 4). The vertical profiles of CH_4 concentrations showed two peaks above 100 mbsf and around 300 mbsf at all sites (Fig. 4c). The C_1/C_2 ratios were approximately 1000 above 900 mbsf at all sites, and decreased below 900 mbsf toward 100 in the deepest part of the core from Site C0002 (Fig. 4d). Hydrocarbons of microbial origin is dominant in CH_4 to other hydrocarbons by more than 1000 (Vogel *et al*., 1982; Belay and Daniels, 1988), indicating that these hydrocarbons are generated by microbial processes. However, when hydrocarbons of thermal origin are migrated upward from great depth, they show the similar ratios. It is necessary to elucidate the stable carbon isotopic compositions of hydrocarbons.

We can differentiate among possible origins and processes of CH_4 in sedimentary environments using several geochemical tools (e.g., Whiticar, 1999). Firstly, we evaluate the C_1/C_2 ratios and the carbon isotope composition of hydrocarbon gases. Furthermore, CO_2 is one carbon end-member species in sediments, and the carbon isotope signatures of CH_4 and CO_2 provide useful information about the source of CH_4. In this study, we elucidate the carbon isotope composition of CH_4 in pore waters from the Nankai accretionary prism off Kumano to gain information about the origin and distribution of CH_4 in these sediments.

Samples

Sediment samples were recovered by the Deep Sea Drilling Vessel (D/V) *Chikyu* on the slope of the Nankai Trough in the accretionary prism during IODP Expeditions 315 and 316 (Kinoshita *et al*., 2009). The cores were retrieved typically in 10.5 m long intervals, and they were segmented into 7 sections of 1.5 m lengths (Table 1). Firstly, about 5 cm^3 volume subsamples of sediment were taken with a plastic syringe cut off the end, or a cork borer for lithified sediments immediately, from a freshly exposed end of each section for determining dissolved hydrocarbon concentrations during Expedition 315. The subsample sediments were subsequently transferred into 20 cm^3 glass serum vials and capped by an aluminum cap with a butyl septum as soon as possible. Meanwhile, during Expedition 316, 3 cm^3 sediment subsamples were taken with a cut-off plastic syringe, or a cork borer for lithified sediments, from a freshly exposed end of each section, and introduced into 20 cm^3 vials containing 10 ml of 4% NaOH to stop all microbial activity. The bottles were sealed by septum as soon as possible, and they were shaken for 2 minutes.

Subsequently, sediment samples for pore water analysis were collected within 1 to 2 h after retrieval. Pore waters were squeezed from the core samples on board the ship by using stainless steel or titanium squeezers (Manheim and Sayles, 1974) immediately after the samples were brought on deck. Samples of about 2 cm^3 intended for carbon isotope ratio analysis of CH_4 and total carbon dioxide ($\sum CO_2$ = CO_2 gas + dissolved CO_2 + HCO_3^- + CO_3^{2-}) were sealed in 3 cm^3 glass bottles with amide sulfuric acid to convert all dissolved carbonate species to CO_2 in the gas phase and $HgCl_2$ as a preservative against microbial activity, and then the vials were immediately capped by an aluminum cap with a butyl rubber septum in the air and stored in darkness. The operation was conducted in the air. The pore waters were also transferred to several bottles for the onboard and onshore measurement of major, minor and trace elements, and several isotopes in onboard and onshore based laboratories.

Analysis

The $\delta^{13}C$ values of CH_4 and $\sum CO_2$ were determined

Fig. 5. Depth profiles of Sites C0001, C0002, C0004, and C0008, from the top to 200 mbsf, showing (a) pore water SO_4^{2-} concentration; (b) pore water CH_4 concentration; (c) $\delta^{13}C$–CH_4 (open squares) and $\delta^{13}C$–$\sum CO_2$ (solid squares); (d) pore water NH_4^+ concentration. The dashed lines in (a) and (c) indicate the depth at which the SO_4^{2-} concentration becomes zero. The dotted lines in (b) and (c) indicate the depth below which the CH_4 concentration becomes low and the $\delta^{13}C$ value becomes constant. Note that the difference in the units of CH_4 concentration: % in the Site C0001 and C0002 profiles and mmol/kg in the Site C0004 and C0008 profiles.

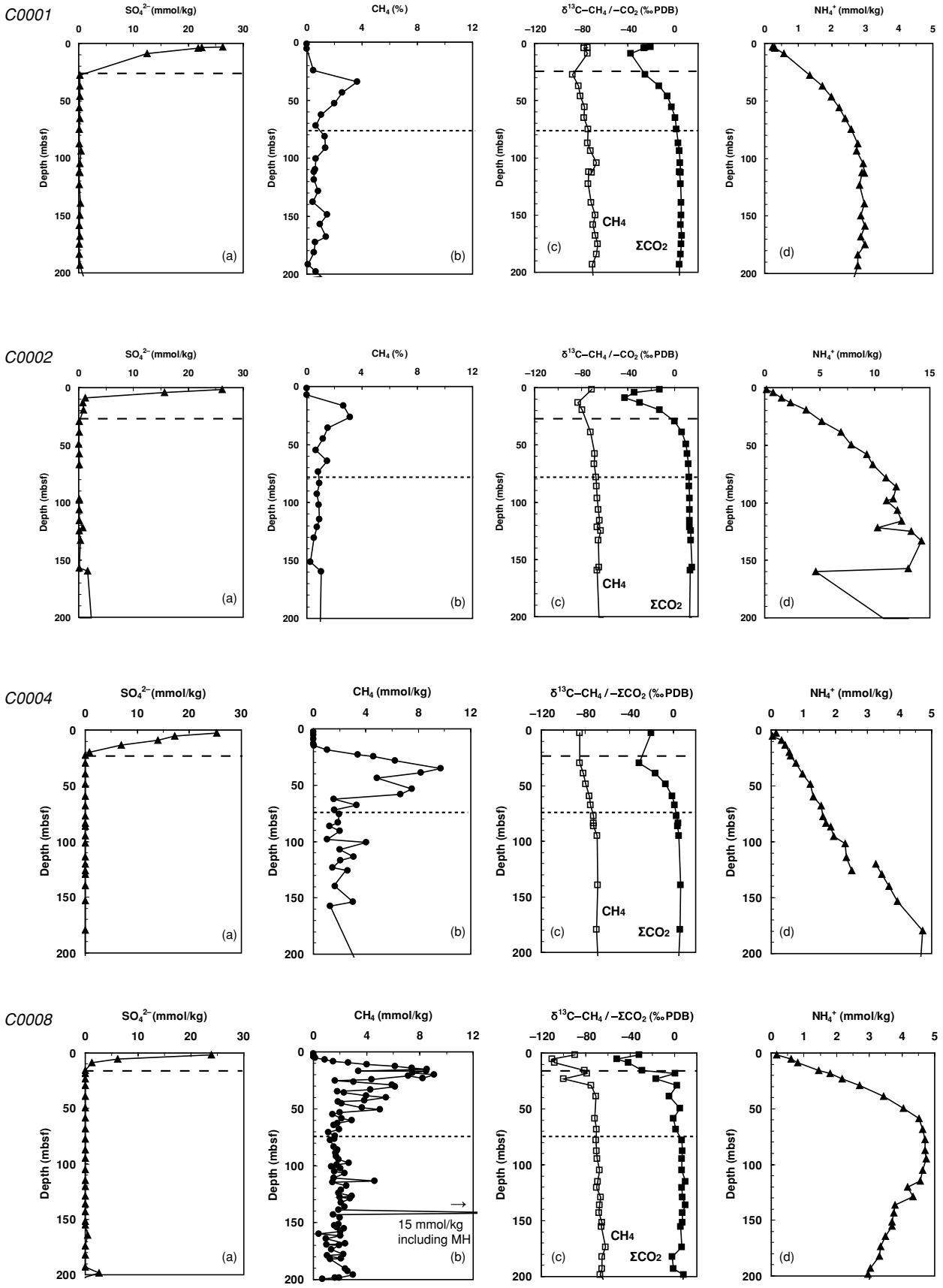
C0001
C0002
C0004
C0008
SO_4^{2-} (mmol/kg)
CH_4 (%)
CH_4 (mmol/kg)
$\delta^{13}C-CH_4$ / $-CO_2$ (‰PDB)
$\delta^{13}C-CH_4$ / $-\Sigma CO_2$ (‰PDB)
NH_4^+ (mmol/kg)
Depth (mbsf)
(a)
(b)
(c)
(d)
CH_4
ΣCO_2
15 mmol/kg
including MH

Fig. 5.

in Hokkaido University by gas chromatography-combustion isotope ratio mass spectrometry using a Finnigan MAT 252 mass spectrometer, and a PoraPLOT Q capillary column (1/32 inch × 25 m) for compound separation (Tsunogai *et al*., 2002; Ijiri *et al*., 2003). The absolute precision of the $\delta^{13}C$ analyses of CH_4 and $\sum CO_2$ was better than ±0.3‰. Stable isotope ratios are reported in the standard delta (δ) notation, in units of permil (‰) relative to PeeDee Belemnite (PDB).

Results

Table 1 lists the results of the $\delta^{13}C$ measurements for CH_4 and $\sum CO_2$. Depth profiles of $\delta^{13}C$–CH_4 and $\delta^{13}C$–$\sum CO_2$ (c) were plotted in Fig. 5 together with (a) SO_4^{2-} concentrations, (b) CH_4 concentrations, and (d) NH_4^+ concentrations reported by Kinoshita *et al*. (2009) in pore water from cores collected at Sites C0001, C0002, C0004, and C0008. In the figure panels, the upper dashed line shows the SO_4^{2-} zero concentration boundary, and the lower dotted line shows the lower boundary of the transition zone to relatively constant $\delta^{13}C$ values of $\sum CO_2$ and CH_4 and to lower CH_4 concentrations.

These vertical profiles show a similar trend at all sites (Fig. 5). CH_4 concentrations increase with depth from around 10 mbsf toward a subsurface peak at approximately 30 to 40 mbsf (Fig. 5b), where the SO_4^{2-} concentration becomes zero (Fig. 5a). The $\delta^{13}C$–CH_4 and $\delta^{13}C$–$\sum CO_2$ values within about 20 to 30 mbsf (Fig. 5c) become decreasing.

Pore water CH_4 concentrations between 10 and 80 mbsf are higher than at the other depths (Fig. 5b). Between 10 and 80 mbsf, the $\delta^{13}C$–CH_4 and $\delta^{13}C$–$\sum CO_2$ values continuously increase with depth, and the relative maximum $\delta^{13}C$ values occur at a depth of approximately 70 to 80 mbsf (Fig. 5c).

Below about 80 mbsf, depth profiles of CH_4 concentrations show a low level at all sites (Fig. 5b). The $\delta^{13}C$–CH_4 values tend to be constant at about –70‰ below 80 mbsf (Fig. 5c). These trends are mirrored in the pore water $\delta^{13}C$–$\sum CO_2$ profiles, which show a constant value of about 0‰ below 80 mbsf in the cores from all four sites (Fig. 5c). The constant $\delta^{13}C$–CH_4 value of –70‰ and $\delta^{13}C$–$\sum CO_2$ value of 0‰ below 80 mbsf extend to the deepest part of the cores at each site except at Site C0002 (Table 1).

The pore water NH_4^+ concentration has a peak around 100 to 150 mbsf (Fig. 5d), suggesting sedimentary organic matter is decomposed by fermentation to short-chain organic compounds, followed by further degradation to CO_2 and NH_4^+ with consequent generation of H_2. Only at Site C0002, the NH_4^+ concentration is higher than the other sites, suggesting that sedimentary organic matter is more highly degraded at only Site C0002.

At Site C0002, which only was drilled up to about 1,000 mbsf, the $\delta^{13}C$–CH_4 value is the highest, –50‰, at 500 mbsf, and it decreases with depth to as low as –60‰ (Table 1). The downhole trend of $\delta^{13}C$–$\sum CO_2$ values is similar to that of $\delta^{13}C$–CH_4 values at Site C0002: the highest $\delta^{13}C$–$\sum CO_2$ value of +15‰ occurs at 500 mbsf and it then becomes increasingly negative downward, eventually reaching –5‰ (Table 1).

Discussion

Contribution of thermogenic methane

We wished to inquire if thermogenic CH_4 may be one source of the CH_4 in the Nankai accretionary prism off Kumano. CH_4 accumulation to generate CH_4 hydrate requires higher rates of *in situ* CH_4 production (Kvenvolden and Barnard, 1983) or higher advective CH_4 fluxes supported by higher rates of fluid migration (Hyndman and Davis, 1992). Contributions of thermogenic CH_4 that have been identified in shallow gas hydrate-bearing sediments of convergent margins have been considered to result from the transport of thermogenic CH_4 along a kind of pathway from greater sediment depths (Whiticar *et al*., 1995; Milkov *et al*., 2005).

To evaluate thermogenic CH_4 contributions, the $\delta^{13}C$ signatures of CH_4 and the C_1/C_2 ratio have been used as diagnostic parameters (Bernard *et al*., 1976): Thermogenic CH_4 is significantly enriched in ^{13}C, and the bulk composition of the gas contains a higher proportion of C_2H_6, than microbial gas (Bernard *et al*., 1976). In isotopic composition, thermogenic CH_4 is usually heavier (more positive) than –50‰ (Sackett, 1978; Seewald *et al*., 1994). Thermogenic gas also has notable quantities of low-molecular-weight hydrocarbons with C_1/C_2 ratios ranging from 0 to 100 (Bernard *et al*., 1976).

In contrast to thermogenic CH_4, microbially derived gas has higher C_1/C_2 ratios than 1000 based on results of experiments using natural sediments and pure cultures (Vogel *et al*., 1982; Belay and Daniels, 1988), which means that the mixture is almost exclusively CH_4. As concerns isotopic composition, microbial hydrogenotrophic methanogenesis produces CH_4 that is highly depleted in ^{13}C as a result of a large isotope fractionation effect that is associated with this biochemical pathway of methanogenesis. It has been shown that isotopic fractionation changes with a hydrogen partial pressure (Valentine *et al*., 2004; Takai *et al*., 2008). A clear correlation has been pointed out to the Gibbs free energy available to hydrogenotrophic methanogens calculated from the Nernst equation (Thauer *et al*., 1977) and isotopic fractionation of a reaction (Penning *et al*., 2005). Within actual marine sediments, a large isotopic fractionation has been reported to range from 50 to 90‰ (Whiticar, 1999; Valentine *et al*., 2004; Penning *et al*.,

2005). $\delta^{13}C$ values of the generated CH_4 are also dependent on $\delta^{13}C$ values of CO_2 as a substrate. The prevailing CO_2 in marine environments is seawater-derived inorganic carbon that has a $\delta^{13}C$ value of about 0‰. Additionally, in marine sediments, CO_2 is generated through degradation of sedimentary organic matter, which has a typical $\delta^{13}C$ value ranging from –25 to –20‰ (Peters *et al*., 1978). The $\delta^{13}C$ values of CH_4 from hydrogenotrophic methanogenesis are more negative than –50‰ (Whiticar, 1999; Valentine *et al*., 2004; Penning *et al*., 2005).

With regard to acetoclastic methanogenesis, $\delta^{13}C$ values of the generated CH_4 depend on isotopic fractionation between $\delta^{13}C$ value of methyl group of acetic acid and $\delta^{13}C$ value of CH_4. It is known that the $\delta^{13}C$ value of methyl group of acetic acid is lower than that of acetic acid itself by about –10 to –5‰ (Blair and Carter Jr., 1992; Conrad *et al*., 2009). The isotopic fractionation has been reported to be a wide range from 7 to 32‰ (Krzycki *et al*., 1987; Blair and Carter Jr., 1992; Valentine *et al*., 2004). Actually, acetoclastic methanogenesis can generate CH_4 with $\delta^{13}C$–CH_4 values between –70‰ and –50‰ observed within natural environments, especially freshwater environments (Whiticar *et al*., 1986).

Figure 6 shows the molecular and isotopic compositions of the gases in pore waters from all sites in this study, together with the compositions of gases previously collected from the Nankai accretionary prism off Muroto (Berner and Faber, 1993) and off Tokai (Waseda and Uchida, 2004). Whereas sampled gases in the MITI well off Tokai clearly have a thermogenic source (Waseda and Uchida, 2004), gases in Hole 808 off Muroto apparently are of mixed origin, consisting of both microbially derived gas and thermogenic gas (Berner and Faber, 1993). The paired $\delta^{13}C$ and C_1/C_2 data obtained in this study indicate mainly microbial sources (Fig. 6). Some data from Site C0002, however, combine an elevated C_1/C_2 ratio with higher $\delta^{13}C$–CH_4 values than the range of microbial sources; these data, which fall outside the expected range of microbial sources, thermogenic sources, and the standard mixing scenario between the two end members (Fig. 6), correspond to the gases from around 500 mbsf (Table 1). These values may have resulted from secondary effects, such as gas oxidation, migration, substrate depletion, and advanced source rock maturity (Coleman *et al*., 1977; Schoell, 1980; Pohlman *et al*., 2009). All samples plot outside of the range of thermogenic sources and indicate thermogenic gas contribution was ruled out (Fig. 6).

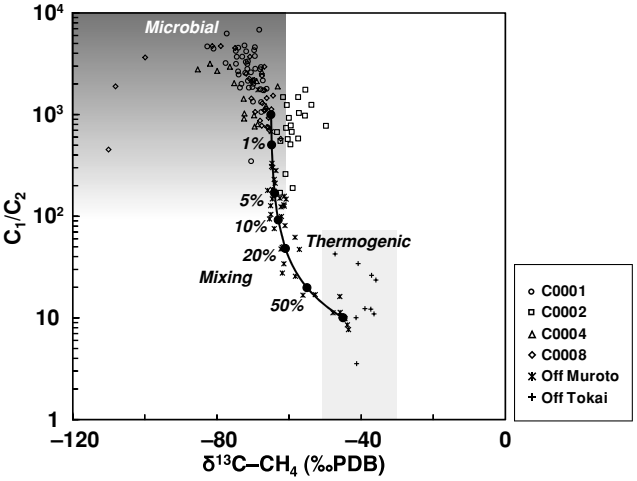

Fig. 6. Relationship between C_1/C_2 and $\delta^{13}C$–CH_4 with respect to gas sources (Bernard et al., 1976) at the four sites, together with the data from Site 808 off Muroto (Berner and Faber, 1993) and the MITI well off Tokai (Waseda and Uchida, 2004). The mixing curve (dashed line) is also shown with contribution ratios of thermogenic end-member, which was calculated by the end-members which can explain data best; microbial end-member (C_1/C_2 = 1000, $\delta^{13}C$–CH_4 = –65‰) and thermogenic end-member (C_1/C_2 = 10, $\delta^{13}C$–CH_4 = –45‰).

Possible methanogenesis pathways

The foregoing discussion has shown that the origin of CH_4 in sediments of the Nankai accretionary prism can be explained by microbial CH_4 production only. Microbial methanogenesis is associated with a kinetic isotope effect (KIE) for carbon that discriminates against ^{13}C. The apparent magnitude of this isotope fractionation varies for different pathways. Methanogenic pathways can be distinguished by examining the stable carbon isotope composition of CH_4 as a function of the co-existing CO_2 (Whiticar, 1999). The isotope separation in δ-notation between two compounds, e.g., $\delta^{13}C$–CH_4 and $\delta^{13}C$–$\sum CO_2$, can be expressed as the isotope separation factor (ε_c):

$$\varepsilon_c \approx \delta^{13}C\text{–}\sum CO_2 - \delta^{13}C\text{–}CH_4. \quad (4)$$

Carbon isotope separation factor between CH_4 and $\sum CO_2$ (ε_c) is generally between 50 and 90 for microbial hydrogenotrophic methanogenesis, while the carbon KIE associated with acetoclastic methanogenesis is lower (ε_c is 40 to 60) (Whiticar, 1999). CH_4 oxidation involves KIE of carbon isotopes that enriches the residual CH_4 in ^{13}C (Alperin *et al*., 1988). The ε_c values related to CH_4 oxidation are generally between 5 and 30 (Whiticar, 1999). Pohlman *et al*. (2009) utilized the isotope separation factor that was proposed by Whiticar (1999) to infer the origin of CH_4 in the Cascadia accretionary prism, and the origin of CH_4 was supported by hydrogen isotope of CH_4 as well as carbon isotope (Pohlman *et al*., 2009).

Figure 7 shows the relationship between co-existing $\delta^{13}C$–CH_4 and $\delta^{13}C$–$\sum CO_2$ values for interpreting gas sources and isotopic shifts resulting from production and

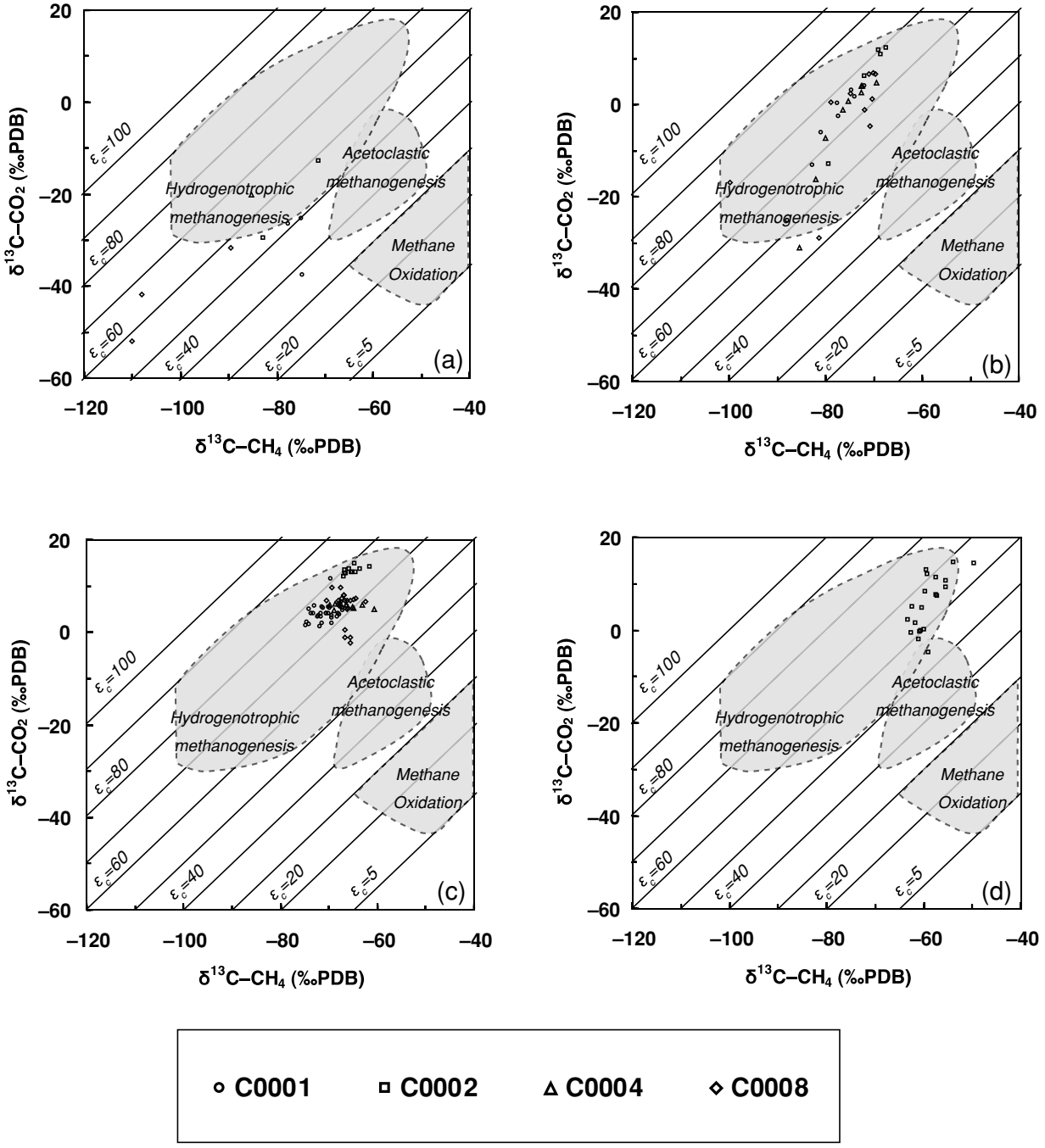

Fig. 7. Relationships between $\delta^{13}C$–CH_4 and $\delta^{13}C$–$\sum CO_2$ with respect to gas sources for four depth intervals: (a) decreasing SO_4^{2-} concentration, (b) abruptly increasing $\delta^{13}C$ values, (c) constant $\delta^{13}C$ values, and (d) below 500 mbsf at only Site C0002. Carbon isotope isofractionation lines (ε_c) calculated with Eq. (4) provided by Whiticar (1999). Methanogenesis by hydrogenotrophic methanogens results in a larger CO_2–CH_4 isotope separation than acetoclastic methanogenesis or CH_4 consumption.

oxidation. The diagonal lines indicate carbon isofractionation lines. The plots show CH_4–$\sum CO_2$ co-existing pairs from the depth interval (a) of decreasing SO_4^{2-} concentration corresponding to the interval above the dashed line in Fig. 5, (b) of abruptly increasing $\delta^{13}C$ values corresponding to the interval between the dashed line and the dotted line in Fig. 5, (c) of constant $\delta^{13}C$ values corresponding to the interval below the dotted line in Fig. 5, and (d) below 500 mbsf at Site C0002 only (Fig. 7).

The CO_2–CH_4 coexisting pairs in the interval where the SO_4^{2-} concentration is decreasing (Fig. 7a) show that the $\delta^{13}C$ values of CH_4 and $\sum CO_2$ fall outside the expected regions of the three processes. The paired $\delta^{13}C$–CH_4 and $\delta^{13}C$–$\sum CO_2$ values are markedly decreasing, indicating coupled anaerobic oxidation of methane (AOM) and methanogenesis (Borowski *et al.*, 1997). AOM is described by Eq. (5) (Reeburgh, 1976; Barnes and Goldberg, 1976; Doose, 1980):

$$CH_4 + SO_4^{2-} \rightarrow HCO_3^- + HS^- + H_2O. \quad (5)$$

The occurrence of AOM is supported by the substantial decrease in SO_4^{2-} (Fig. 5a). The isotopic ratio of $\sum CO_2$ within this AOM zone is significantly lower than that of marine organic matter, because ^{13}C-depleted CH_4 that is produced microbially below the AOM zone diffuses upward into the AOM zone (Suess and Whiticar, 1989). Subsequent cycling of ^{13}C-depleted $\sum CO_2$ into the CH_4 pool by microbial hydrogenotrophic methanogenesis creates progressively more ^{13}C-depleted CH_4 (Borowski *et al.*, 1997), as shown by values as low as –110‰ in our data (Fig. 7a). Thus, the distributions of $\delta^{13}C$ values of CH_4 and $\sum CO_2$ in the surface sediments are interpreted to reflect a combination of microbially mediated processes: anaerobic methane oxidation and hydrogenotrophic methanogenesis. Extremely negative $\delta^{13}C$–CH_4 and $\delta^{13}C$–$\sum CO_2$ values in the AOM zone are observed in all cores, suggesting that coupled AOM and hydrogenotrophic methanogenesis is a widespread phenomenon in the Nankai accretionary prism off Kumano.

In the interval of abruptly increasing $\delta^{13}C$ values (Fig. 7b), both $\delta^{13}C$–CH_4 and $\delta^{13}C$–$\sum CO_2$ values become higher along the $\sum CO_2$–CH_4 isofractionation line corresponding to microbial hydrogenotrophic methanogenesis, that is, ε_c about 70 to 80. This relationship suggests a linkage between the CH_4 and $\sum CO_2$ pools via microbial hydrogenotrophic methanogenesis. The shift to more ^{13}C-enriched values of CH_4 and $\sum CO_2$ is related to preferential use of ^{12}C during microbial hydrogenotrophic methanogenesis (Galimov and Kvenvolden, 1983; Claypool *et al.*, 1985). As light carbon isotope in $\sum CO_2$ is preferentially transferred to CH_4, the residual $\sum CO_2$ pool is left relatively enriched with ^{13}C; thus, subsequent CH_4 formation from this $\sum CO_2$ pool accentuates the trend of ^{13}C-enriched CH_4 formation. As shown in Fig. 7a, some microbial hydrogenotrophic methanogenesis occurs prior to complete consumption of SO_4^{2-} in the surface sediments, but sulfate-reducing bacteria out-compete methanogens for H_2 and acetate (Abram and Nedwell, 1978; Ferry and Lessner, 2008); after SO_4^{2-} reduction is completed, only methanogenesis occurs in the sediments (e.g., Claypool and Kaplan, 1974; Martens and Berner, 1974; Whiticar, 1999). This relationship leads to the well-known biogeochemical stratification of dissolved constituents in the pore fluids of marine sediments in which the methanogenic zone underlies the SO_4^{2-}-reducing zone (Claypool and Kaplan, 1974). Sites C0001, C0002, C0004, and C0008 display this typical biogeochemical zonation of dissolved constituents with a shallow SO_4^{2-} reduction zone and a deeper methanogenic zone.

In the interval with constant $\delta^{13}C$ values (Fig. 7c), both $\delta^{13}C$–CH_4 and $\delta^{13}C$–$\sum CO_2$ values are relatively constant at ε_c in the range of 70 and 80, which typically indicates microbial hydrogenotrophic methanogenesis in marine sediments (Whiticar, 1999). However, the constant $\delta^{13}C$–CH_4 and $\delta^{13}C$–$\sum CO_2$ values with depth indicate that methanogenic *Archaea* are inactive below 100 mbsf in these cores, because the KIE during microbial hydrogenotrophic methanogenesis should lead to progressive enrichment the residual CO_2 with ^{13}C, as a result CH_4 produced from this carbon substrate enrich in ^{13}C (Claypool *et al.*, 1985). This interpretation is supported by the depth profiles of CH_4 concentrations, which show a low level in this depth interval (Fig. 5b). Additionally, the constant $\delta^{13}C$–$\sum CO_2$ values suggests that it is unlikely that organic matter decomposition occurs in the sedimentary section below 100 mbsf at all sites, because the microbial breakdown of organic compounds, fermentation, in anoxic environments should yield CO_2 with a low $\delta^{13}C$ value similar to that of sedimentary organic matter contained in the Nankai accretionary prism (–20.5‰: Omura and Ikehara, 2010). These results suggest that microbial activity is totally inactive in this interval.

Below 500 mbsf at Site C0002 (Fig. 7d), ε_c decreases to 65 compared to the ε_c value of ~75 at other depths, and the $\delta^{13}C$–CH_4 and $\delta^{13}C$–$\sum CO_2$ values become lower with increasing depth while ε_c remains relatively constant. This shift suggests that in this depth interval the additional input of CO_2 resulting from degradation of organic matter with a $\delta^{13}C$ value similar to that of organic matter in this area ($\delta^{13}C$ = –20.5‰: Omura and Ikehara, 2010) becomes the dominant process, instead of methanogenesis, which because of the KIE would lead to a shift to heavier values. The clear linkage between $\delta^{13}C$–CH_4 and $\delta^{13}C$–$\sum CO_2$ values in this depth interval indicates at least the occurrence of methanogenesis with CO_2 as the precursor.

Consumption of the initial $\sum CO_2$ pool by methanogenesis

In all intervals, hydrogenotrophic methanogenesis is a dominant process of CH_4 generation, so that we will access a degree of methanogenesis activity assuming a closed system to the accretionary prism. Even though the natural environment is an open system, the closed-system distillation model of Rayleigh allows us to estimate approximately the magnitude of methanogenesis activity (Rayleigh, 1896). Assuming a closed system, the ^{13}C enrichment in $\sum CO_2$ and CH_4 is generally described

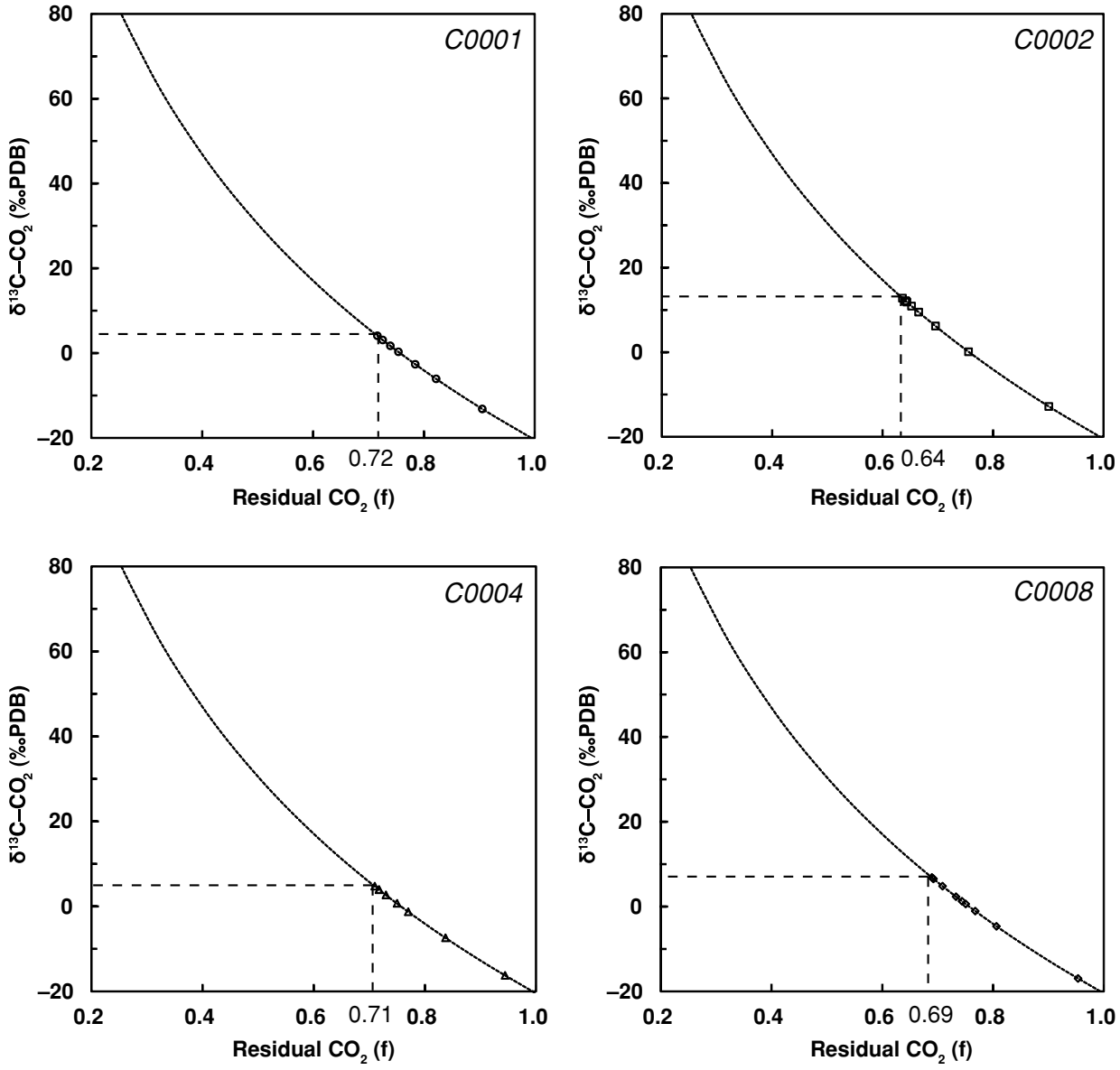

Fig. 8. Relationships between $\delta^{13}C$–$\sum CO_2$ to ratios of the residual CO_2 from CH_4 production (Eq. (7)).

by the distillation function of Rayleigh (1896), simplified by using ε_c (Whiticar, 1999),

$$\delta^{13}C\text{–}\sum CO_{2,t} - \delta^{13}C\text{–}\sum CO_{2,i} = -\varepsilon_c \ln f \quad (6)$$

$$\delta^{13}C\text{–}CH_{4,t} - \delta^{13}C\text{–}\sum CO_{2,i} = -\varepsilon_c(1 + \ln f). \quad (7)$$

$\delta^{13}C$–$\sum CO_{2,t}$ and $\delta^{13}C$–$CH_{4,t}$ are the isotopic compositions of the residual $\sum CO_2$ and the accumulating CH_4 product, respectively, at time t. The ratio f is the fraction of initial $\sum CO_2$ remaining at time t. $\delta^{13}C$–$\sum CO_{2,i}$ is the initial isotope ratio of the precursor CO_2, and can be approximated by the $\delta^{13}C$ value of sedimentary organic carbon, –20.5‰, the representative value in the Nankai accretionary prism off Kumano (Omura and Ikehara, 2010). As the fraction f of the initial substrate $\sum CO_2$ pool decreases, $\delta^{13}C$–$\sum CO_{2,t}$ and $\delta^{13}C$–$CH_{4,t}$ values progressively shift toward ^{13}C-enriched values.

We evaluate the fraction $(1 - f)$ of the initial substrate $\sum CO_2$ pool converted to CH_4 by hydrogenotrophic methanogenesis using Eqs. (6) and (7) and the average $\delta^{13}C$–CH_4 and $\delta^{13}C$–$\sum CO_2$ values between 100 and 200 mbsf at each site for $\delta^{13}C$–$CH_{4,t}$ and $\delta^{13}C$–$\sum CO_{2,t}$, respectively (Fig. 8). The results indicate the conversion of ~30% of the initial $\sum CO_2$ to CH_4 at Sites C0001, C0004, and C0008, and ~36% at Site C0002. Thus, at Site C0002

a larger fraction of the initial substrate $\sum CO_2$ pool has been consumed by hydrogenotrophic methanogenesis at the sediment depth of 100 to 200 m.

Potential methanogenesis in the Kumano Basin

Contents of total organic carbon (TOC) in sediments from all sites are approximately constant at ~0.4 wt% (Kinoshita *et al*., 2009), and therefore cannot explain the different fraction of the initial $\sum CO_2$ pool consumed by hydrogenotrophic methanogenesis at Site C0002. TOC content is thus not the major factor controlling the magnitude of hydrogenotrophic methanogenesis. The sedimentation rate ranged from 140 to 180 m/m.y. at Site C0001, and from 400 to 800 m/m.y. at Site C0002 (Kinoshita *et al*., 2009). The sedimentation rates at Sites C0004 and C0008 have not been reported, but biostratigraphic ages based on nannofossils and foraminifers have been reported for all sites drilled during Expeditions 315 and 316 (Kinoshita *et al*., 2009). According to the biostratigraphic results, the age of the sediment at 100 mbsf is 1.5 Ma at Site C0001, 1 Ma at Site C0002, 3 Ma at Site C0004, and 1.5 Ma at Site C0008. The rate of sedimentation therefore may have been relatively low at Sites C0001, C0004 and C0008 compared to the rate at Site C0002. In addition, the pore water NH_4^+ concentration increases with depth to a maximum value at ~100 mbsf in all cores: 3 mM at Site C0001, 11 mM at Site C0002, 3 mM at Site C0004, and 5 mM at Site C0008 (Fig. 5d; Kinoshita *et al*., 2009). The higher NH_4^+ concentration at Site C0002 compared to the other sites indicates that the organic matter is more highly degraded, and this degradation would supply CO_2 and H_2 as substrates for methanogenesis, which could lead to greater methanogenic activity.

When sedimentation rates are enough high, organic matter is buried without aerobic degradation due to decreasing the exposed time to oxygen on the surface of the seafloor (Canfield, 1994). The residual labile organic matter is useful to anaerobic processes, including sulfate reduction and hydrogenotrophic methanogenesis (Penning and Conrad, 2007). Actually, the sedimentation rates are above 400 m/m.y. at Site C0002 and below 200 m/m.y. at the other sites, corresponding to the threshold value of 300 m/m.y. shown in Canfield (1994). In addition, on the slope of the accretionary prism, slope sediments are intermittently collapsed and deposited again along the slope (Sakaguchi *et al*., 2011). Such sediments would have been exposed to organic matter degradation anaerobically in the subsurface as well as aerobically on the surface of the seafloor, which already have been poor in labile and useful organic matter for microbial processes. Accordingly, useful organic matter for supporting CH_4 production leaves scant in the slope sediments.

At Site C0002, the high sedimentation rate thus led to active degradation of organic matter, stimulated microbial metabolism, and supported higher CH_4 production. The high sedimentation rate fundamentally reflects the geographical factor of distance from land, and also the geomorphological factor of the site's location inside the outer ridge that rims the sediment-filled Kumano Basin. The outer ridge acts as a sill and reduces sediment flow out from the forearc basin. Indeed, the Kumano Basin is filled with sediments 2 to 3 km thick according to seismic reflection images, whereas the landward slope is covered by a thin sediment that slides down toward the toe of the prism (Moore *et al*., 2009; Strasser *et al*., 2009). As a result of this geomorphological setting, the potential source of CH_4 hydrates would be higher in sediments in the Kumano Basin than in those on the Nankai accretionary prism slope off Kumano; thus, geomorphology was an important factor controlling CH_4 formation and accumulation at Site C0002.

Conclusion

During IODP Expeditions 315 and 316, a four-site transect (Sites C0001, C0002, C0004, and C0008) was drilled in the Nankai accretionary prism off Kumano (Kinoshita *et al*., 2009). Only Site C0002 is located in the forearc basin, whereas the other sites are located on the slope of the Nankai accretionary prism. A vast and thick CH_4 hydrate layer occurs at Site C0002 at ~400 mbsf (Kinoshita *et al*., 2008). We address CH_4 formation and accumulation in sediments using the isotopic composition of CH_4 and the hydrocarbon composition in the pore water from all four sites in conjunction with the isotopic composition of the co-existing CO_2. These data indicate that thermogenic CH_4 is not a significant source of CH_4 in the shallow sediments of the Nankai accretionary prism off Kumano.

The magnitude of the carbon isotope separation between CH_4 and CO_2 suggests that microbial hydrogenotrophic methanogenesis is the predominant CH_4 source at all investigated sites. Calculations of the fraction of the initial substrate CO_2 pool converted to CH_4 showed that a larger fraction is consumed by methanogenesis at Site C0002 than at the other sites along the transect off Kumano. Although the reported TOC contents were similar at all four sites, the sedimentation rate was distinctively higher at Site C0002 compared with the rates at the other sites (Kinoshita *et al*., 2009). In addition, the NH_4^+ concentrations at Site C0002 are also higher than those reported from the other sites (Kinoshita *et al*., 2009), indicating more organic matter degradation activity at Site C0002 than at the other sites.

The high sedimentation rate at Site C0002 is primarily attributed to its geographical location (distance from land), and to its geomorphological position within the

outer ridge rimming the forearc basin, leading to a difference of preservation of organic matter for methanogenesis. Geomorphology can be an important factor controlling CH_4 formation and accumulation in marine environments, and the Kumano Basin has more potential as a reservoir of CH_4 hydrates than the Kumano landward slope.

Acknowledgments—The authors would like to thank the ship's crew, drilling personnel, staff, and technicians aboard the D/V *Chikyu*, and the sample collection personnel at the Center for Deep Earth Exploration (CDEX). We are grateful to NanTroSEIZE chief project scientists, specialty coordinators, and the scientists of Expeditions 315 and 316. We are also grateful to J. M. Gieskes and S. Kawagucci for their critical comments and constructive suggestions for improvement of an earlier version of this manuscript. This research was funded by the Ministry of Education, Culture, Sports, Science and Technology (MEXT), Japan, through a special coordination fund (KANAME Project: New perspective of great subduction-zone earthquakes from super-deep drilling).

REFERENCES

Abram, J. W. and Nedwell, D. B. (1978) Inhibition of methanogenesis by sulphate reducing bacteria competing for transferred hydrogen. *Arch. Microbiol.* **117**, 89–92.

Alperin, M. J., Reeburgh, W. S. and Whiticar, M. J. (1988) Carbon and hydrogen isotope fractionation resulting from anaerobic methane oxidation. *Global Biogeochem. Cycles* **2**, 279–288.

Barnes, R. O. and Goldberg, E. D. (1976) Methane production and consumption in anoxic marine sediments. *Geology* **4**, 297–300.

Belay, N. and Daniels, L. (1988) Ethane production by Methanosarcina barkeri during growth in ethanol supplemented medium. *Antonie Van Leeuwenhoek* **54**, 113–125.

Bernard, B. B., Brooks, J. M. and Sackett, W. M. (1976) Natural gas seepage in the Gulf of Mexico. *Earth Planet. Sci. Lett.* **31**, 48–54.

Berner, U. and Faber, E. (1993) Light hydrocarbons in sediments of the Nankai accretionary prism (Leg 131, Site 808). *Proceedings of the Ocean Drilling Program, Scientific Results* **131** (Hill, I. A., Taira, A., Firth, J. V. *et al*., eds.), 185–195, Ocean Drilling Program, College Station.

Blair, N. E. and Carter, W. D., Jr. (1992) The carbon isotope biogeochemistry of acetate from a methanogenic marine sediment. *Geochim. Cosmochim. Acta* **56**, 1247–1258.

Borowski, W. S., Paull, C. K. and Ussler, W. (1997) Carbon cycling within the upper methanogenic zone of continental rise sediments; An example from the methane-rich sediments overlying the Blake Ridge gas hydrate deposits. *Mar. Chem.* **57**, 299–311.

Canfield, D. E. (1994) Factors influencing organic carbon preservation in marine sediments. *Chem. Geol.* **114**, 315–329.

Cappenberg, T. E. and Prins, R. A. (1974) Interrelations between sulfate-reducing and methane-producing bacteria in bottom deposits of a fresh water lake III. Experiments with carbon-14-labeled substrates. *Antonie Van Leeuwenhoek* **40**, 457–469.

Claypool, G. E. and Kaplan, I. R. (1974) The origin and distribution of methane in marine sediments. *Methane in Marine Sediments* (Kaplan, I. R., ed.), 99–139, Plenum Press.

Claypool, G. E., Threlkeld, C. N., Mankiewicz, P. N., Arthur, M. A. and Anderson, T. F. (1985) Isotopic composition of interstitial fluids and origin of methane in slope sediment of the Middle America trench, Deep-Sea Drilling Project Leg-84. *Initial Reports of the Deep Sea Drilling Project* **84** (von Huene, R., Aubouin, J. *et al*., eds.), 683–691, U.S. Government Printing Office.

Claypool, G. E., Vuletich, A. K. and Kvenvolden, K. A. (1986) Isotopic composition of interstitial fluids in sediment of the Nankai Trough. *Initial Reports of the Deep Sea Drilling Project* **87** (Kagami, H., Karig, D. E., Coulboum, W. T. *et al*., eds.), 857–860, U.S. Government Printing Office.

Coleman, D. D., Meents, W. F., Lin, C. and Keogh, R. A. (1977) Isotopic identification of leakage gas from underground storage reservoirs—a progress report. *Illinois State Geological Survey. Illinois Petroleum* **111**, 1–10.

Conrad, R., Claus, P. and Casper, P. (2009) Characterization of stable isotope fractionation during methane production in the sediment of a eutrophic lake, Lake Dagow, Germany. *Limnol. Oceanogr.* **54**, 457–471.

Dickens, G. R., Castillo, M. M. and Walker, J. C. G. (1997) A blast of gas in the latest Paleocene: Simulating first-order effects of massive dissociation of oceanic methane hydrate. *Geology* **25**, 259–262.

Doose, P. R. (1980) *The Bacterial Production of Methane in Marine Sediments*. Univ. of California, 240 pp.

Egeberg, P. K. and Dickens, G. R. (1999) Thermodynamic and pore water halogen constraints on gas hydrate distribution at ODP Site 997 (Blake Ridge). *Chem. Geol.* **153**, 53–79.

Fehn, U., Snyder, G. and Egeberg, P. K. (2000) Dating of Pore Waters with ^{129}I: Relevance for the Origin of Marine Gas Hydrates. *Science* **289**, 2332–2335.

Ferry, J. G. and Lessner, D. J. (2008) Methanogenesis in marine sediments. *Incredible Anaerobes: From Physiology to Genomics to Fuels* (Wiegel, J., Maier, R. J. and Adams, M. W. W., eds.), 147–157, Blackwell.

Galimov, E. M. and Kvenvolden, K. A. (1983) Concentrations and carbon isotopic compositions of CH_4 and CO_2 in gas from sediments of the Blake Outer Ridge, Deep Sea Drilling Project, Leg 76. *Initial Reports of the Deep Sea Drilling Project* **76** (Shipley, T. H., Orlofsky, S. *et al*., eds.), 403–407, U.S. Government Printing Office.

Hesse, R. and Harrison, W. E. (1981) Gas hydrates (clathrates) causing pore-water freshening and oxygen isotope fractionation in deep-water sedimentary sections of terrigenous continental margins. *Earth Planet. Sci. Lett.* **55**, 453–462.

Heuer, V. B., Pohlman, J. W., Torres, M. E., Elvert, M. and Hinrichs, K.-U. (2009) The stable carbon isotope biogeochemistry of acetate and other dissolved carbon species in deep subseafloor sediments at the northern Cascadia Margin. *Geochim. Cosmochim. Acta* **73**, 3323–3336.

Hungate, R. E. (1967) Hydrogen as an intermediate in the rumen fermentation. *Archiv fuer Mikrobiologie* **59**, 158–164.

Hyndman, R. D. and Davis, E. E. (1992) A mechanism for the

formation of methane hydrate and seafloor bottom-simulating reflectors by vertical fluid expulsion. *J. Geophys. Res.* **97**, 7025–7041.

Ijiri, A. (2003) Stable isotopic studies on fluid and gas migration in forearc sediments. Ph.D. Thesis, Hokkaido University, 100 pp.

Ijiri, A., Tsunogai, U. and Gamo, T. (2003) A simple method for oxygen-18 determination of milligram quantities of water using $NaHCO_3$ reagent. *Rapid Communications in Mass Spectrometry* **17**, 1472–1478.

Jeris, J. S. and McCarty, P. L. (1965) The biochemistry of methane fermentation using ^{14}C tracers. *Journal—Water Pollution Control Federation* **37**, 178–192.

Kennett, J., Cannariato, K. G., Hendy, I. L. and Behl, R. J. (2003) *Methane Hydrates in Quaternary Climate Change. The Clathrate Gun Hypothesis*. AGU, 216 pp.

Kinoshita, M., Tobin, H., Moe, K. T. and the Expedition 314 Scientists (2008) NanTroSEIZE Stage 1A: NanTroSEIZE LWD transect. *Integrated Ocean Drilling Program Expedition 314 Preliminary Report* **314**, 1–63.

Kinoshita, M., Tobin, H., Ashi, J., Kimura, G., Lallement, S., Screaton, E. J., Curewitz, D., Masago, H., Moe, K. T. and the Expedition 314/315/316 Scientists (2009) Expedition 316 summary. *Proceedings of the Integrated Ocean Drilling Program Expeditions* **314/315/316** (Kinoshita, M., Tobin, H., Ashi, J. *et al*., eds.), Integrated Ocean Drilling Program Management International, Inc.

Krzycki, J. A., Kenealy, W. R., Deniro, M. J. and Zeikus, J. G. (1987) Stable carbon isotope fractionation by methanosarcina-barkeri during methanogenesis from acetate, methanol, or carbon dioxide-hydrogen. *Appl. Environ. Microbiol.* **53**, 2597–2599.

Kvenvolden, K. A. (1988) Methane hydrate—A major reservoir of carbon in the shallow geosphere? *Chem. Geol.* **71**, 41–51.

Kvenvolden, K. A. (1993) Gas hydrates-geological perspective and global change. *Rev. Geophys.* **31**, 173–187.

Kvenvolden, K. A. and Barnard, L. A. (1983) Gas hydrates of the Blake Outer Ridge, Site 533. *Initial Reports of the Deep Sea Drilling Project* **76** (Sheridan, R. E., Gradstein, F. *et al*., eds.), 353–365, U.S. Government Printing Office.

Kvenvolden, K. A. and Kastner, M. (1990) Gas hydrates of the Peruvian outer continental margin. *Proceedings of the Ocean Drilling Program, Scientific Results* **112** (Suess, E., von Huene, R. *et al*., eds.), 517–526.

Lovley, D. R. and Klug, M. J. (1986) Model for the distribution of sulfate reduction and methanogenesis in freshwater sediments. *Geochim. Cosmochim. Acta* **50**, 11–18.

Maekawa, T. and Imai, N. (2000) Hydrogen and oxygen isotope fractionation in water during gas hydrate formation. *Gas Hydrates: Challenges for the Future* (Holder, G. D. and Bishnoi, P. R., eds.), 452–459, Annals New York Academy Sciences.

Malinverno, A., Kastner, M., Torres, M. E. and Wortmann, U. G. (2008) Gas hydrate occurrence from pore water chlorinity and downhole logs in a transect across the northern Cascadia margin (Integrated Ocean Drilling Program Expedition 311). *J. Geophys. Res.* **113**, B08103.

Manheim, F. T. and Sayles, F. L. (1974) Composition and origin of interstitial waters of marine sediments, based on deep sea drill cores. *The Sea* **5**, 527–568.

Martens, C. S. and Berner, R. A. (1974) Methane production in the interstitial waters of sulfate-depleted marine sediments. *Science* **185**, 1167–1169.

Milkov, A. V., Claypool, G. E., Lee, Y. J. and Sassen, R. (2005) Gas hydrate systems at Hydrate Ridge offshore Oregon inferred from molecular and isotopic properties of hydratebound and void gases. *Geochim. Cosmochim. Acta* **69**, 1007–1026.

Mitchell, J. B. F. (1989) The "greenhouse" effect and climate change. *Rev. Geophys.* **27**, 115–139.

Moore, G. F., Taira, A., Klaus, A., Becker, L., Boeckel, B., Cragg, B. A., Dean, A., Fergusson, C. L., Henry, P., Hirano, S., Hisamitsu, T., Hunze, S., Kastner, M., Maltman, A. J., Morgan, J. K., Murakami, Y., Saffer, D. M., Sánchez-Gómez, M., Screaton, E. J., Smith, D. C., Spivack, A. J., Steurer, J., Tobin, H. J., Ujiie, K., Underwood, M. B. and Wilson, M. (2001) New insights into deformation and fluid flow processes in the Nankai Trough accretionary prism: Results of Ocean Drilling Program Leg 190. *Geochem. Geophys. Geosyst.* **2**, 1058.

Moore, G. F., Park, J.-O., Bangs, N. L., Gulick, S. P., Tobin, H. J., Nakamura, Y., Saito, S., Tsuji, T., Yoro, T., Tanaka, H., Uraki, S., Kido, Y., Sanada, Y., Kuramoto, S. and Taira, A. (2009) Structural and seismic stratigraphic framework of the NanTroSEIZE Stage 1 transect. *Proceedings of the Integrated Ocean Drilling Program* **314/315/316** (Kinoshita, M., Tobin, H., Ashi, J. *et al*., eds.), 1–46, Integrated Ocean Drilling Program Management International, Inc.

Omura, A. and Ikehara, K. (2010) Deep-sea sedimentation controlled by sea-level rise during the last deglaciation, an example from the Kumano Trough, Japan. *Mar. Geol.* **274**, 177–186.

Oremland, R. S. and Polcin, S. (1982) Methanogenesis and sulfate reduction: Competitive and noncompetitive substrates in estuarine sediments. *Appl. Environ. Microbiol.* **44**, 1270–1276.

Oremland, R. S., Marsh, L. M. and Polcin, S. (1982) Methane production and simultaneous sulphate reduction in anoxic, salt marsh sediments. *Nature* **296**, 143–145.

Park, J.-O., Tsuru, T., Kodaira, S., Cummins, P. R. and Kaneda, Y. (2002) Splay fault branching along the Nankai subduction zone. *Science* **297**, 1157–1160.

Penning, H. and Conrad, R. (2007) Quantification of carbon flow from stable isotope fractionation in rice field soils with different organic matter content. *Org. Geochem.* **38**, 2058–2069.

Penning, H., Plugge, C. M., Galand, P. E. and Conrad, R. (2005) Variation of carbon isotope fractionation in hydrogenotrophic methanogenic microbial cultures and environmental samples at different energy status. *Global Change Biol.* **11**, 2103–2113.

Peters, K. E., Sweeney, R. E. and Kaplan, I. R. (1978) Correlation of carbon and nitrogen stable isotope ratios in sedimentary organic matter. *Limnol. Oceanogr.* **23**, 598–604.

Pohlman, J. W., Kaneko, M., Heuer, V. B., Coffin, R. B. and Whiticar, M. (2009) Methane sources and production in the northern Cascadia margin gas hydrate system. *Earth Planet.*

Sci. Lett. **287**, 504–512.
Quigley, T. M. and Mackenzie, A. S. (1988) The temperatures of oil and gas formation in the sub-surface. *Nature* **333**, 549–552.
Rayleigh, J. W. S. (1896) Theoretical considerations respecting the separation of gases by diffusion and similar processes. *Philos. Mag.* **42**, 493–498.
Reeburgh, W. S. (1976) Methane consumption in Cariaco Trench waters and sediments. *Earth Planet. Sci. Lett.* **28**, 337–344.
Sackett, W. M. (1978) Carbon and hydrogen isotope effects during the thermocatalytic production of hydrocarbons in laboratory simulation experiments. *Geochim. Cosmochim. Acta* **42**, 571–580.
Sakaguchi, A., Kimura, G., Strasser, M., Screaton, E. J., Curewitz, D. and Murayama, M. (2011) Episodic seafloor mud brecciation due to great subduction zone earthquakes. *Geology* **39**, 919–922.
Schoell, M. (1980) The hydrogen and carbon isotopic composition of methane from natural gases of various origins. *Geochim. Cosmochim. Acta* **44**, 649–661.
Seewald, J. S., Seyfried, W. E., Jr. and Shanks Iii, W. C. (1994) Variations in the chemical and stable isotope composition of carbon and sulfur species during organic-rich sediment alteration: An experimental and theoretical study of hydrothermal activity at guaymas basin, gulf of California. *Geochim. Cosmochim. Acta* **58**, 5065–5082.
Seno, T., Stein, S. and Gripp, A. E. (1993) A model for the motion of the Philippine Sea plate consistent with NUVEL-1 and geological data. *J. Geophys. Res.* **98**, 17941–17948.
Shipley, T. H., Houston, M. H., Buffler, R. T., Shaub, F. J., McMillen, K. J., Ladd, J. W. and Worzel, J. L. (1979) Seismic evidence for widespread possible gas hydrate horizons on continental slopes and rises. *AAPG Bull.* **63**, 2204–2213.
Smith, P. H. and Mah, R. A. (1966) Kinetics of acetate metabolism during sludge digestion. *Appl. Microbiol.* **14**, 368–371.
Strasser, M., Moore, G. F., Kimura, G., Kitamura, Y., Kopf, A. J., Lallemant, S., Park, J.-O., Screaton, E. J., Su, X., Underwood, M. B. and Zhao, X. (2009) Origin and evolution of a splay fault in the Nankai accretionary wedge. *Nature Geosci.* **2**, 648–652.
Suess, E. and Whiticar, M. J. (1989) Methane-derived CO_2 in pore fluids expelled from the Oregon subduction zone. *Palaeogeogr., Palaeoclimatol., Palaeoecol.* **71**, 119–136.
Takai, K., Nakamura, K., Toki, T., Tsunogai, U., Miyazaki, M., Miyazaki, J., Hirayama, H., Nakagawa, S., Nunoura, T. and Horikoshi, K. (2008) Cell proliferation at 122°C and isotopically heavy CH_4 production by a hyperthermophilic methanogen under high-pressure cultivation. *Proceedings of the National Academy of Sciences* **105**, 10949–10954.
Thauer, R. K., Jungermann, K. and Decker, K. (1977) Energy conservation in chemotrophic anaerobic bacteria. *Microbiol. Mol. Biol. Rev.* **41**, 100–180.
Toki, T., Tsunogai, U., Gamo, T., Kuramoto, S. and Ashi, J. (2004) Detection of low-chloride fluids beneath a cold seep field on the Nankai accretionary wedge off Kumano, south of Japan. *Earth Planet. Sci. Lett.* **228**, 37–47.
Tsunogai, U., Yoshida, N. and Gamo, T. (2002) Carbon isotopic evidence of methane oxidation through sulfate reduction in sediment beneath cold seep vents on the seafloor at Nankai Trough. *Mar. Geol.* **187**, 145–160.
Ussler, W. and Paull, C. K. (1995) Effects of ion exclusion and isotopic fractionation on pore water geochemistry during gas hydrate formation and decomposition. *Geo-Mar. Lett.* **15**, 37–44.
Valentine, D. L., Chidthaisong, A., Rice, A., Reeburgh, W. S. and Tyler, S. C. (2004) Carbon and hydrogen isotope fractionation by moderately thermophilic methanogens. *Geochim. Cosmochim. Acta* **68**, 1571–1590.
Vogel, T. M., Oremland, R. S. and Kvenvolden, K. A. (1982) Low-temperature formation of hydrocarbon gases in San Francisco Bay sediment (California, U.S.A.). *Chem. Geol.* **37**, 289–298.
Waseda, A. and Uchida, T. (2004) Origin and migration of methane in gas hydrate-bearing sediments in the Nankai Trough. *The Geochemical Society Special Publications* **9** (Hill, R. J., Leventhal, J., Aizenshtat, Z. *et al.*, eds.), 377–387, Elsevier.
Wellsbury, P., Goodman, K., Barth, T., Cragg, B. A., Barnes, S. P. and Parkes, R. J. (1997) Deep marine biosphere fuelled by increasing organic matter availability during burial and heating. *Nature* **388**, 573–576.
Whiticar, M. J. (1999) Carbon and hydrogen isotope systematics of bacterial formation and oxidation of methane. *Chem. Geol.* **161**, 291–314.
Whiticar, M. J., Faber, E. and Schoell, M. (1986) Biogenic methane formation in marine and freshwater environments: CO_2 reduction vs. acetate fermentation—Isotope evidence. *Geochim. Cosmochim. Acta* **50**, 693–709.
Whiticar, M. J., Hovland, M., Kastner, M. and Sample, J. C. (1995) Organic geochemistry of gases, fluids, and hydrates at the Cascadia accretionary margin. *Proceedings of the Ocean Drilling Program, Scientific Results* **146** (Pt. 1) (Carson, B., Westbrook, G. K., Musgrave, R. J. *et al.*, eds.), 385–397, Ocean Drilling Program, College Station.
Xu, W. and Ruppel, C. (1999) Predicting the occurrence, distribution, and evolution of methane gas hydrate in porous marine sediments. *J. Geophys. Res.* **104**, 5081–5095.